SENSITIVITY AND UNCERTAINTY ANALYSIS OF THE SCWR CORE ALONG ITS CYCLE WITH THE INCLUSION OF CONTROL BLADES AND BURNABLE ABSORBERS

J. R. Sharpe[1], A. Buijs[1]
[1]McMaster University, Hamilton, Ontario, Canada
sharpejr@mcmaster.ca, buijsa@mcmaster.ca

Abstract

The assessment of nuclear reactor uncertainties has long been a topic of study, and is becoming increasingly important in the safety and economical design of nuclear power plants. Integral response uncertainties, such as Δk_{eff}, can be computed using adjoint-based perturbation theory which has been implemented in KENO/TSUNAMI. The underlying nuclide and reaction sensitivities and uncertainties in the SCWR core with the inclusion of control blades and burnable absorbers, over a cycle, were the topic of study for this paper. Full core SCWR KENO models at various burnups were generated using TRITON to produce lattice burnups with control blade branches and PARCS to determine core wide burnup evolution and control blade insertions. The highest sensitivities as well as uncertainties in the SCWR core were found to be plutonium reactions. It was also found that Δk_{eff} decreases slightly throughout the cycle from 0.84 to 0.8 $\Delta k/k$.

1. Introduction

The uncertainty associated with integral quantities, such as Δk_{eff}, is becoming of growing interest for critical systems. This paper will study Δk_{eff} for the SCWR along its cycle, and in doing so will study the sensitivities and uncertainties contributions of important nuclides and their reactions.

Knowledge of the uncertainty on k_{eff} and other integral responses is crucial when designing a new critical system or power reactor such as the SCWR for a number of reasons, namely:

1. Economically, for example the uncertainty bounds of the cycle length,
2. Safety, for example in calculating the uncertainty in reactivity coefficients, and
3. Proliferation, for example in knowing the quantities of plutonium remaining in the fuel after its final cycle.

The safety case is the main reason for performing uncertainty calculations on integral quantities. For example, if a reactor's coolant void reactivity (CVR) is calculated to be -1 mk, presumably it's safe for the coolant to be voided. However, an uncertainty analysis may reveal a CVR of -1 ± 4 mk. This is important because the delayed neutron fraction (beta) of the SCWR at the beginning of cycle is ~3 mk. Thus, an accident scenario that voids the coolant may push the reactor into the prompt critical regime. This extreme (and unlikely) case demonstrates the importance of understanding uncertainties.

Integral response uncertainties originate from the uncertainties in the underlying nuclear data. The details of their calculation will be introduced in the following sections. However, once the

uncertainty analysis has been performed for a given core or critical system, the next step would be to attempt to reduce the uncertainties in quantities like k_{eff}. There is a technique that can be used to reduce the uncertainties, however, it is an in-depth procedure consisting of experimental results from existing critical facilities and the detailed modelling and simulation of these experimental facilities. If there is a sufficient number of experiments that are similar to the reactor in question (in this case the SCWR), knowledge of those experiments can be used to reduce the uncertainty on the SCWR's simulated responses (i.e. Δk_{eff}).

In addition to simply finding the uncertainty on important integral quantities, the analysis itself also identifies which nuclides, reactions, and energy groups contribute to those uncertainties, and the reactivity sensitivity of the reactor to those nuclides/reactions/energy groups. A brief explanation is given below for the important steps in the analysis.

1.1 Sensitivity

The sensitivity of k with respect to the nuclear data α, is defined as [1]:

$$S_{k,\alpha} = \frac{\alpha}{k}\frac{dk}{d\alpha} \qquad (1)$$

The nuclear data, α, can be a macroscopic cross section, Σ; the fission distribution, χ; or the number of neutrons per fission, υ. Each type of nuclear data may have an associated isotope, i; reaction, x; or energy group, g.

The adjoint-based perturbation method is used to determine these sensitivities. This method requires the forward and adjoint flux solutions in all energy groups and regions of the reactor. This step is performed by KENO V.a [2] which is included in the SCALE 6.1 package [3]. KENO is a multigroup, or continuous energy, stochastic transport code capable of modelling the SCWR core. Once the adjoint-based technique is applied, Equation (1) can be shown to take the form [4]:

$$S_{k,\Sigma} = \frac{\Sigma}{k}\frac{\partial k}{\partial \Sigma} = -\frac{\Sigma}{k}\frac{\langle \phi^* \left| \frac{\partial A(\Sigma)}{\partial \Sigma} - \lambda \frac{\partial B(\Sigma)}{\partial \Sigma} \right| \phi \rangle}{\langle \phi^* | \lambda B(\Sigma) | \phi \rangle} \qquad (2)$$

Where A is an operator representing all the terms in the transport equation except for fission terms, and B represents all the fission terms. λ is the fundamental eigenvalue equal to k^{-1}, and finally, ϕ and ϕ^* are the forward and adjoint flux, respectively.

The sensitivity analysis module for SCALE (SAMS) is then used to calculate the sensitivities of all the nuclides, reactions and energy groups in the problem. These sensitivities are then put into the form of a vector, $\boldsymbol{S_k}$ of length $i \times x \times g$.

1.2 Uncertainty

The variance of k_{eff} with respect to nuclear data uncertainties can be calculated as follows [4]:

$$\sigma_k^2 = \boldsymbol{S_k C_{\alpha\alpha} S_k^T} \qquad (3)$$

where $\boldsymbol{S_k^T}$ is the transpose of $\boldsymbol{S_k}$ and $\boldsymbol{C_{\alpha\alpha}}$ is the covariance matrix of the nuclear data. $\boldsymbol{C_{\alpha\alpha}}$ contains all the relative variances and covariances between all nuclides, reactions and energy groups used to describe the KENO model of the SCWR. It is included in the TSUNAMI package for uncertainty analyses. As mentioned above, the uncertainty contribution of each nuclide, reaction and energy group can be found. This is important in deriving which nuclides should be further investigated to provide more accurate cross section data.

2. Methodology

The main focus of this paper is to ascertain Δk_{eff}, the major uncertainty contributors to Δk_{eff}, and also the important nuclide and reaction sensitivities throughout the SCWR cycle. The procedure used to achieve the goal of this study involves a lattice model of the SCWR fuel in NEWT, a quarter core SCWR model in PARCS and a quarter core SCWR model in KENO. A description of a PARCS-to-KENO model generator will also be given.

2.1 Fuel Lattice (TRITON)

The modified Canadian SCWR fuel lattice is shown in Figure 1. It consists of 64 fuel pins and 32 burnable absorbers with a cruciform control blade that is inserted in the moderator between four fuel lattices. Details of the fuel lattice's components, dimensions, and composition can be found in [5]. The inner fuel pins are 15 wt % PuO_2/ThO_2 and the outer pins are slightly larger in dimension with a 12 wt % PuO_2/ThO_2 composition, with a lattice pitch of 25 cm. A notable difference between this lattice and that documented in [5] is the absence of integrated burnable absorbers in the fuel and the addition of the Excel Zirconium Alloy control blades [6], using SS304 as the absorbing material. The burnable absorbers [7], are located in the insulator and are composed of natural gadolinium. The specific compositions of these altered components are found in Table 1.

The fuel lattice was first modelled in NEWT [8] and was depleted using TRITON [9]. NEWT is a 2D multigroup transport code using the extended step characteristics approach to solve the transport equation. TRITON depletes the materials in the cell and calls upon NEWT to solve the transport equation in order to find the fluxes at each step.

Component	Dimension	Material	Composition (wt %)	Density (g/cm^3)
Burnable Absorbers	0.06 cm radius 7.525 cm pitch circle radius (evenly spaced, $\pi/32$ offset)	Natural Gadolinium	Gd-(152: 0.2%; 154: 1.9%; 155: 13.3%; 156: 18.6%; 157: 22.6%; 158: 23.1%; 160: 20.3%)	7.90
Control Blade (Cruciform shaped)	Structure length: 24.2 cm, width: 0.5 cm.	Structure: Excel (Zirc. Alloy)	Structure: Zr: 94.9%; Nb: 0.8%; Mo: 0.8%; Sn: 3.5%	6.52
	Absorber length: 13 cm, width: 0.2 cm, origin: (x,y)=(11, 0) cm	Absorber: SS304s	Absorber: C: 0.08%; Si: 1%; P-31: 0.045%; Cr: 19%; Mn-55: 2%; Fe: 68.375%; Ni: 9.5%	7.94

Table 1: Geometry and Composition specifications for the modified Canadian SCWR fuel lattice cell.

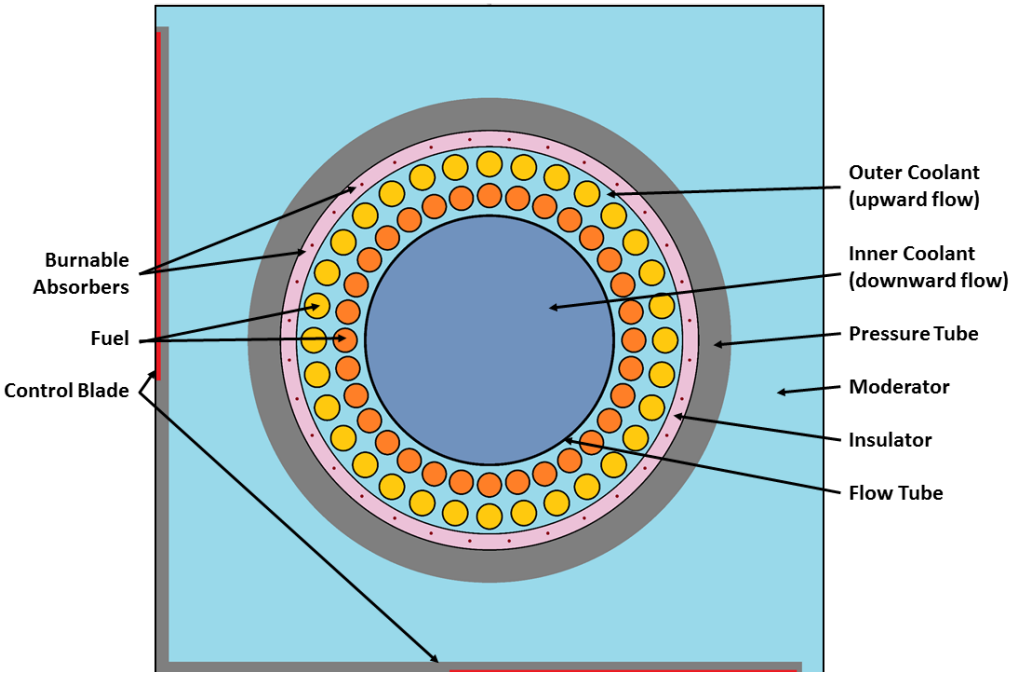

Figure 1: The modified Canadian SCWR Fuel Lattice with a cruciform control blade and burnable absorbers.

The average lattice power was 47.282 MW/MTIHM (Megawatt per metric ton of initial heavy metal) and was depleted, beginning with fresh fuel, to a final burnup of 68.6 MW/MTIHM. In total there were 103 burnup steps and at each step homogenized and condensed two-group cross sections were produced, to be used later in the full core diffusion code PARCS [10].

2.2 Quarter Core (PARCS)

PARCS [10] is a diffusion code which uses the finite difference method to solve the diffusion equation for the one-quarter SCWR core. It is also capable of determining the insertion depth of control devices in order to maintain criticality. PARCS was used in two-group mode for this study.

The SCWR core has average individual assembly powers of 7.56 MW to make a whole-core thermal power of 2540 MW. The fuel region in the core is 5.0 m in height, with 1.0 m of nominal radial reflectors, and 0.75 m of axial reflector on the top and bottom of the core. Each channel is cooled by light water and the surrounding moderator is heavy water. The three-batch shuffling scheme and additional core details can be found in [11] and [5], respectively. A top view of the quarter SCWR core is shown in Figure 2.

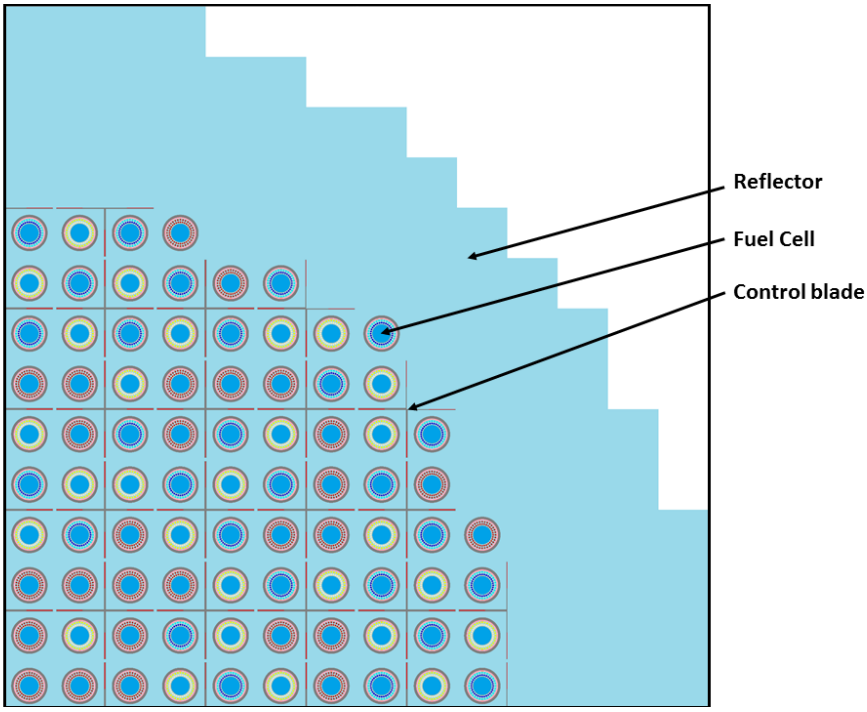

Figure 2: SCWR Quarter Core including cruciform control blades.

Neither ADFs (Assembly Discontinuity Factors) nor multi-cell exact cross sections were included in the diffusion calculation due to insufficient literature on the effects of ADFs on SCWR calculations. It has been shown that multi-cell exact cross sections result in an improvement in assembly powers predicted by diffusion codes when compared to stochastic codes [12]. Unfortunately the method of calculating exact cross sections was not possible with the tools available to perform this study.

2.3 PARCS to KENO model generator

A model generator script was developed using Python in order to produce a KENO model with the appropriate depleted compositions. The quarter-core-wide burnups, having 10 axial nodes in 84 assemblies (providing 840 nodes), were found using PARCS. Those burnups were interpolated from the NEWT composition outputs to find the interpolated compositions of each of the 840 nodes to be placed into the KENO model. These burnup interpolations were performed for the inner fuel pins, outer fuel pins, and burnable absorbers. This leads to one composition for each of the two rings of fuel, and the burnable absorbers, at each of the ten axial locations.

Having 840 individual burnup compositions in KENO was not possible as the code cannot handle such a large number of nuclides. To work around this, each of the ten axial positions was allowed to have three different compositions, one for each fuel batch, the calculation of which is discussed below. The reason each axial position was chosen to have a unique set of three compositions is that there are significant differences in the neutronics at each axial position due to changes in coolant densities, coolant temperature, and fuel temperature (demonstrated in [13]).

The PARCS output is not binned in any way, and produces $84 \times 10 = 840$ unique burnups. In order to reduce this to $84 \times 3 = 252$ unique burnups all nodes' burnups were plotted in a histogram (at each axial position, individually) with 0.1 MWd/kg wide bins. A Gaussian distribution was then fitted to

each of the three batches of fuel, in each axial position, producing 252 Gaussians distributions. The mean of each Gaussian was used as the nominal burnup for each of the three batches in each of the ten axial positions. Bins with 1 MWd/kg width and fitted Gaussians are shown in Figure 3.

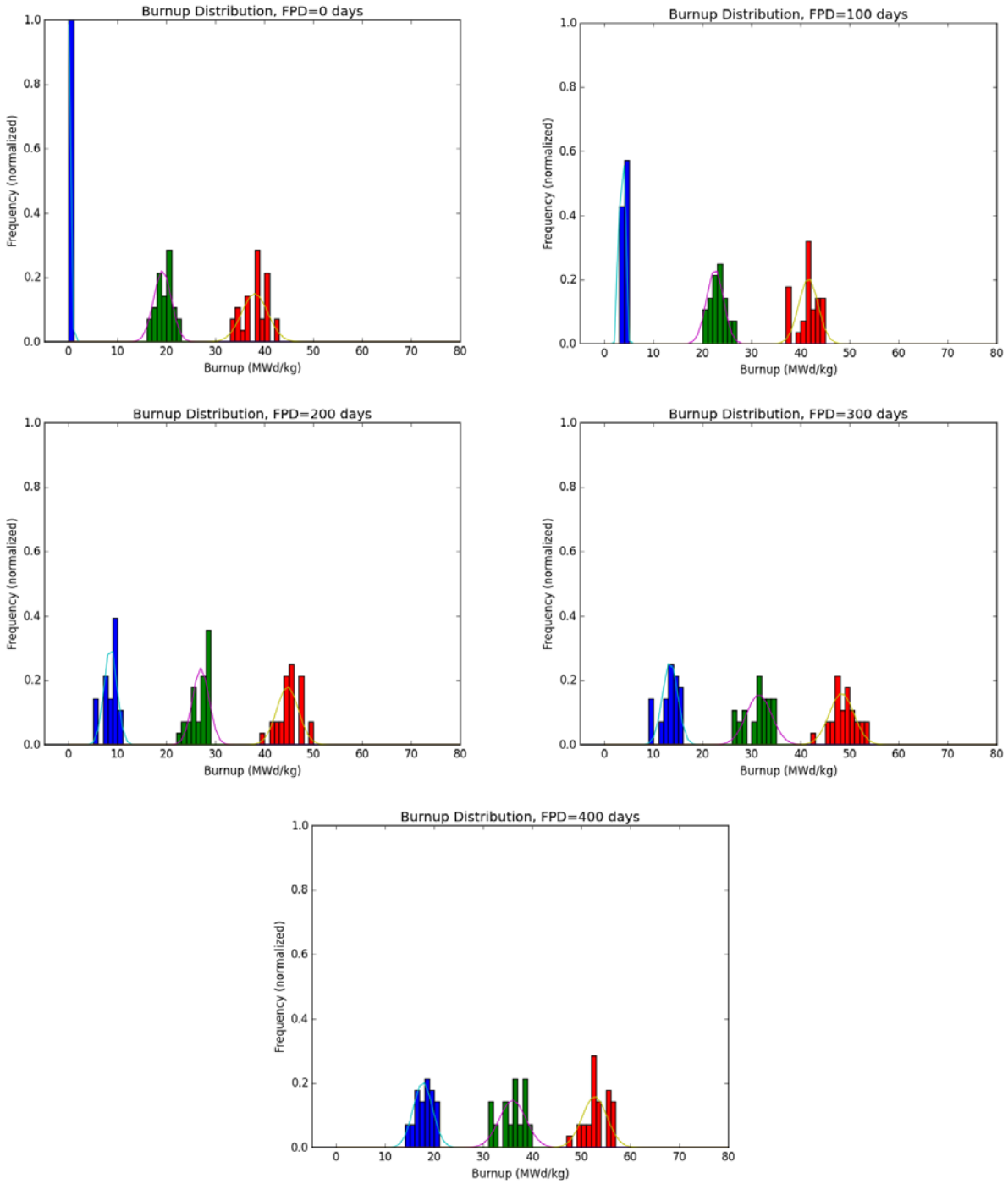

Figure 3: Burnup distribution and evolution along the SCWR cycle.

Note the shift to the right for all three batches as the number of FPD (full power days) increases. In addition to the obvious shift, there is also a widening of each grouping of node burnups. This is most obvious for fresh fuel, however also occurs for the second and third batch.

When TRITON produces the composition files at each depletion step, there are 388 nuclides in each file. However, again, due to computational limits it was not possible to include all 388 nuclides for each KENO node. Rather, all nuclides with a number density less than 10^{-6} $cm^{-2} \cdot b^{-1}$ were removed resulting in roughly ~50 to ~100 remaining nuclides. Ideally, each nuclide with an insignificant cross section would be removed; however, the above method has been shown to produce essentially identical results as using all 388 nuclides [14].

The PARCS simulation code includes a module to find an equilibrium core for a given shuffling scheme. The shuffling scheme [6] used in this study was not optimized for burnable absorbers or control blades as that was not the goal of this study. However, the flux is sufficiently flat such that sensitivities should not be significantly changed by optimizing the shuffling scheme.

An equilibrium core was first found without the use of control blades with a cycle length of 428 days, then a control blade sequence was found that kept the core above $k_{eff} = 1.01$. This slight excess reactivity accounts for any additional structures and detectors in the core that were not considered in this study. A second equilibrium core was then found which included the control blade sequence found prior. The cycle length with control blades for the second equilibrium core was 420 days in order to keep $k_{eff} > 1.01$. A second control blade sequence was then found which maintained $k_{eff} > 1.01$, resulting in a cycle length of 404 days, which is the reference core for this study. The core-wide burnup values from the 840 nodes of the reference core, along with the control blade insertions, were used as the starting point for the above description of choosing the nominal burnups of the three batches at each of the ten axial positions.

All sensitivity and uncertainty analysis was completed using the TSUNAMI-3D [15] tool included in the SCALE package. It used KENO to solve the transport problem in 238 groups and SAMS to calculate the sensitivities and uncertainties.

3. Results

3.1 k_{eff}

The primary goal of this study was to find Δk_{eff} along the cycle for each k_{eff} and is shown in Figure 4. Recall that the k_{eff} calculated by PARCS was "forced" to be 1.01 along the vast majority of the cycle extracting control blade banks, one at a time. The KENO results presented are calculated from only an approximation of the burnups in PARCS, as described above, and this is most likely the cause of the discrepancies between the two k_{eff} lines (however, this has not been tested). The deviation at the beginning of the cycle is due to differences in the Xe and Sm loads and how they are calculated in PARCS and TRITON. In Figure 4 the k_{eff} for PARCS has a data point at each day, whereas the KENO data points are indicated on the graph.

3.2 Sensitivity

When investigating sensitivities, it is possible to gain insight as to what is occurring in the core at a more fundamental level. Changes can be seen including shifts in the importance of nuclides' and reactions' throughout the cycle.

Figure 5 shows the nuclides/reactions to which k_{eff} is the most sensitive. These sensitivities are energy-group, region, and mixture integrated. The nuclides/reactions with the highest sensitivity are: ^{239}Pu $\bar{\nu}$, ^{239}Pu fission, ^{239}Pu capture, ^{241}Pu $\bar{\nu}$, and ^{241}Pu fission. This is expected considering they are the major sources of neutrons in the core. In order to cause a fission, a neutron must first be captured, therefore, the magnitude of ^{239}Pu capture is also large but, by contrast, its value is negative since neutron captures reduce k_{eff}. From the way this graph is plotted, there do not appear to be any major changes in the nuclides with the highest sensitivities.

Figure 6 shows the nuclide/reaction sensitivities that change the most over the cycle (if their sensitivity is >5 x 10^{-3}). They reveals how the core evolves over time. The data shown in Figure 6 is represented by Equation 4:

$$y = \frac{S(t) - S(t=0)}{|S(t=0)|} \tag{4}$$

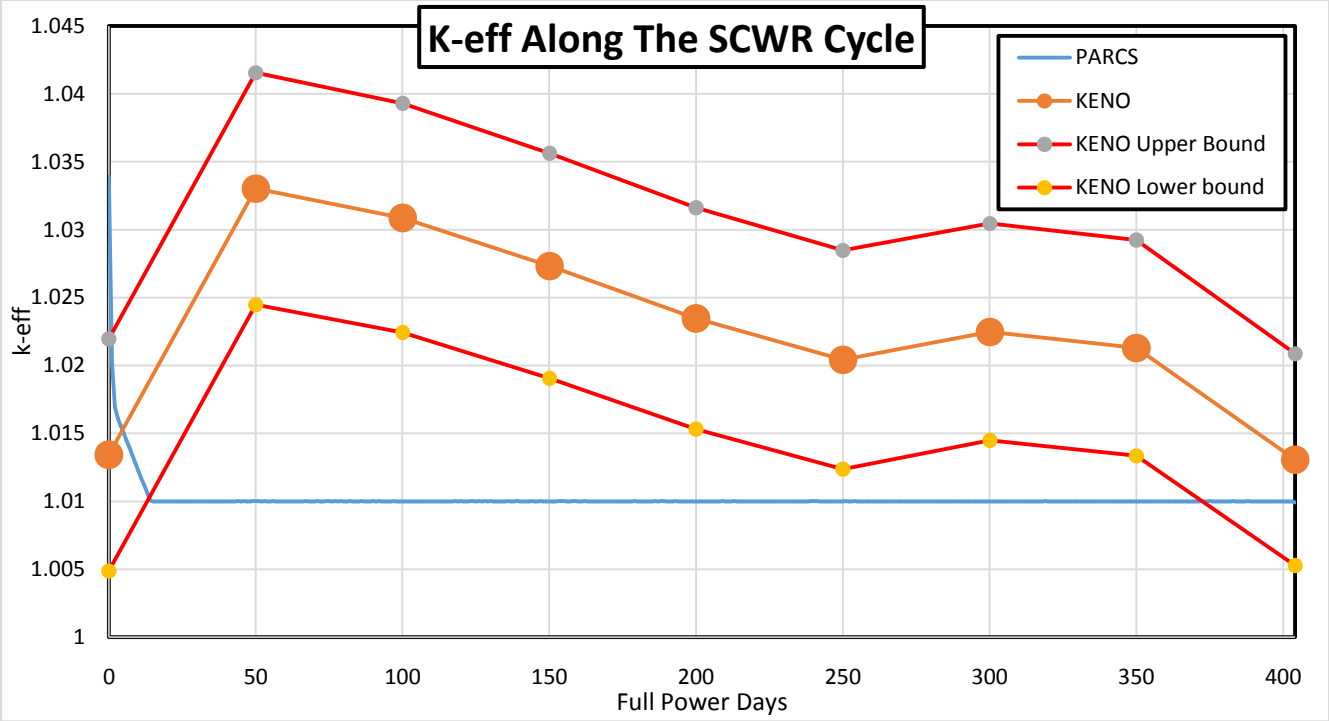

Figure 4: A comparison of PARCS and KENO calculated k_{eff} along the SCWR cycle. The uncertainty bars are due to uncertain nuclear data.

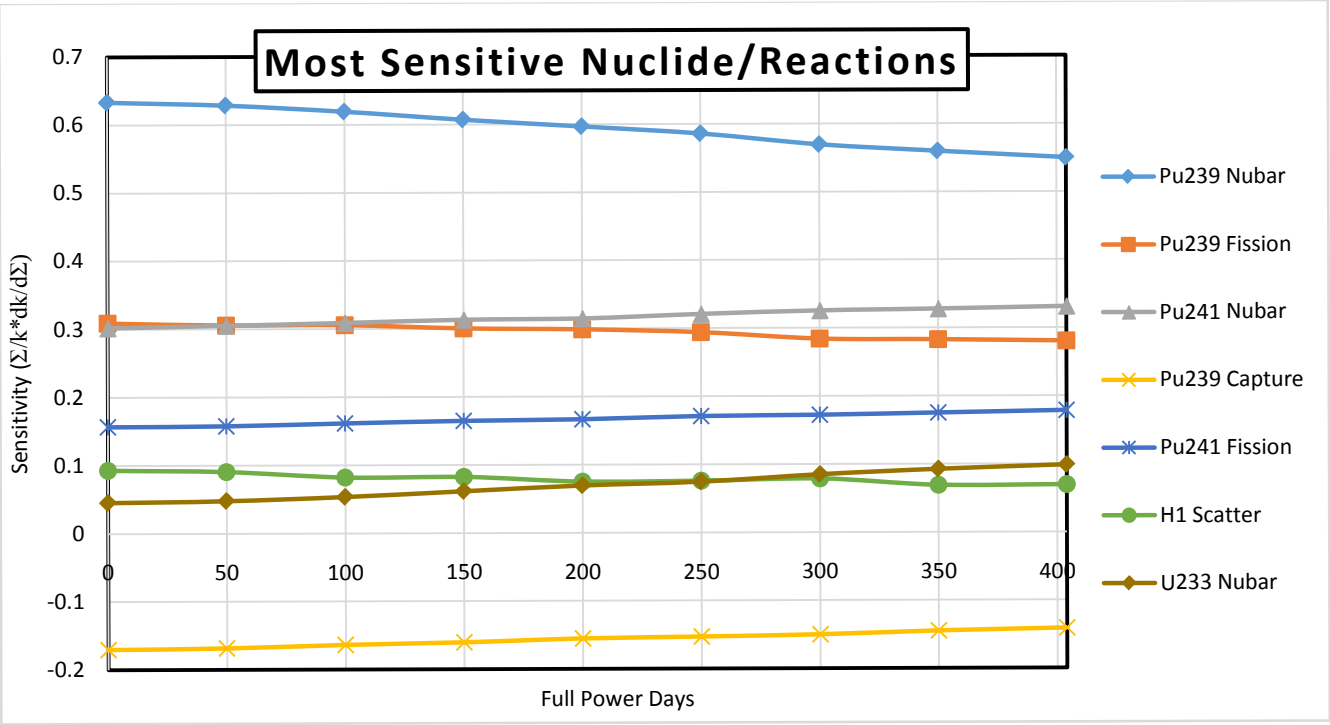

Figure 5: The 10 most sensitive nuclides/reactions throughout the cycle.

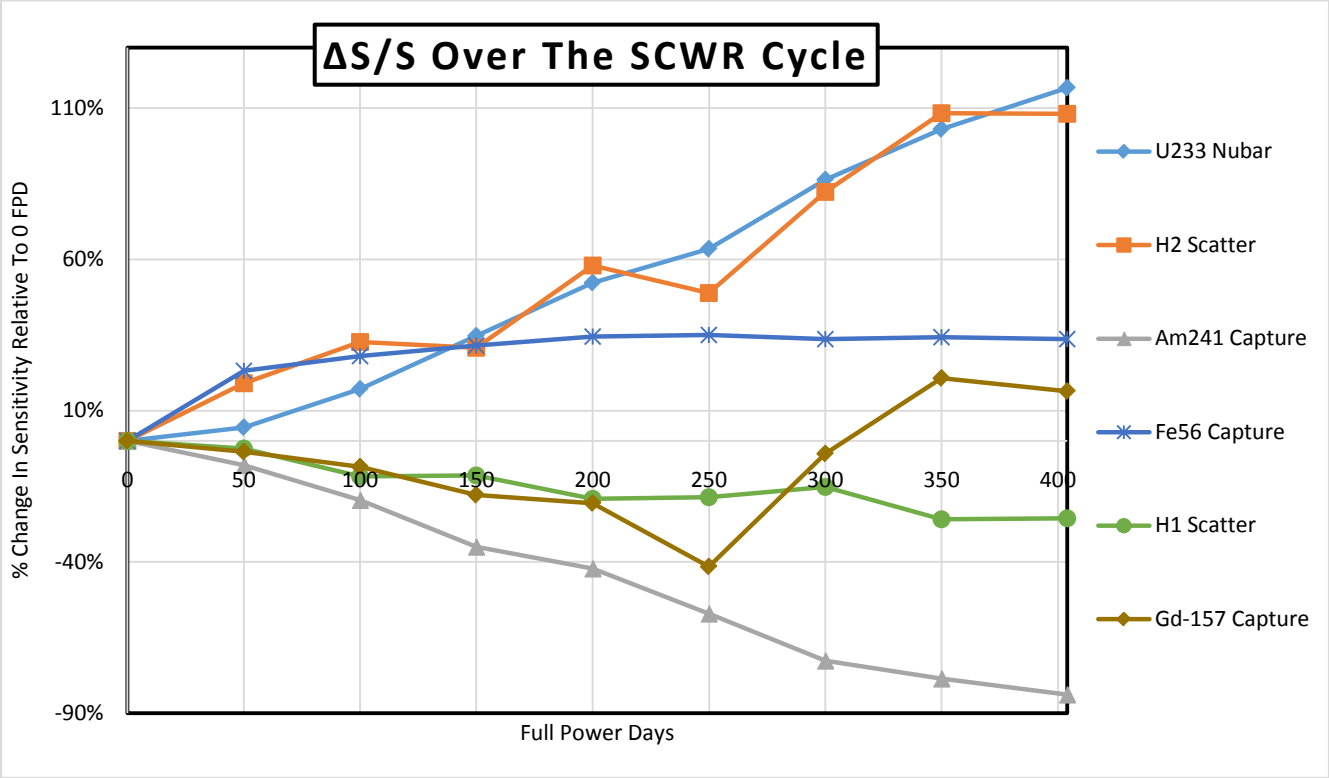

Figure 6: Relative changes in sensitivity of some of the most sensitive nuclides and reactions over the course of the SCWR cycle.

where y are the plotted values, S(t) are the sensitivities at time t, and S(t=0) are the initial sensitivities at FPD=0. Equation 4 represents the relative change in sensitivity at each step compared to the beginning of cycle (0 FPD). It is with this data that the evolution of the cycle can be dissected.

In the KENO models of the SCWR quarter core, control blades are initially fully inserted in the core to suppress reactivity, then are slowly withdrawn, one bank at a time, from the periphery inwards, as reactivity is needed to maintain criticality. This can be seen on the graph by ^{56}Fe capture decreasing throughout the cycle due to the absorbing portion of the blades being composed of 68.375% Fe (as shown in Table 1). This is mimicked by the decrease in ^{53}Cr capture sensitivity (not shown in Figure 6) as Cr makes up 19% of the control blades absorber material. The magnitude of the ^{53}Cr capture is not as large as the ^{56}Fe capture mainly because there is significantly more ^{56}Fe in the blades.

Since the control blades are placed between fuel lattices in the moderator, fewer neutrons are absorbed in the moderator region (by the blades) and moderation by ^{2}H is increased significantly, as the blades are withdrawn, as shown in Figure 6. The decreased absorption by ^{56}Fe and ^{53}Cr, and the increased moderation of ^{2}H, as the blades are removed represent a portion of the reactivity worth of the blades and also where that reactivity worth originates. More specifically, it is not only a reduction in absorption cross section but also an increase in moderation that contributes to lowering their reactivity worths. The sensitivity of ^{16}O also increases in part due to the blades being withdrawn, since heavy water (D_2O) is the moderator.

^{233}U $\bar{\nu}$ (not shown in Figure 6) and ^{233}U fission sensitivities increase throughout the cycle, due to fertile ^{232}Th being transmuted into ^{233}U. A large increase in the ^{233}U $\bar{\nu}$ and ^{233}U fission sensitivities on this graph should not be confused with the actual relatively small value of the ^{233}U $\bar{\nu}$ and ^{233}U fission sensitivities shown in Figure 5. This indicates that although both sensitivities have a large relative increase, they are still only a fraction of the other sensitivities listed in Figure 5.

^{239}Pu capture starts negative in Figure 5 and becomes less negative, this is reflected in Figure 6 because the fissile Pu is being depleted over the course of the cycle. The same is true for ^{238}Pu capture. In contrast, ^{241}Am is a by-product of the Pu nuclear chain reaction, and builds up over the cycle. This causes an increase in its capture sensitivity.

^{157}Gd capture has a more obscure explanation, but consists of a combination of: (1) the Gd depleting throughout the cycle, (2) the power peak shifting from the periphery of the core to the centre of the core as the cycle progresses, and (3) the distribution of first, second, and third cycle fuel in the refuelling scheme.

3.3 Uncertainty

The uncertainty contribution of nuclide/reaction pairs to k_{eff} is calculated from Equation (3). Whereas sensitivities are only contributed from "varying" a single nuclide/reaction cross section, uncertainties can arise from a single nuclear/reaction, called a variance, and also from the combination of two different nuclide reactions, called a covariance. This arises from a shared uncertainty between two nuclides/reactions/energy groups.

The most important contributors to the uncertainty of k_{eff} are shown in Figure 7. The variance of ^{239}Pu $\bar{\nu}$ is the largest uncertainty contributor, this is due to (1) the large amount of ^{239}Pu in the core, and (2) the experimental difficulty in accurately measuring $\bar{\nu}$. In addition, when a single fuel type (in this case primarily plutonium) keeps a reactor critical any small change in $\bar{\nu}$ will have a large impact on k_{eff}. Note the absence of ^{233}U fission, absorption or $\bar{\nu}$ in Figure 7, this is because ^{233}U has a small sensitivity compared to the other significant uncertainty contributors. In addition, in the thermal energy region, ^{233}U has a fission $\Delta\sigma/\sigma$ equal to ~1/3 that of ^{239}Pu [16].

4. Discussion

This paper should be treated as a preliminary investigation into the sensitivities and uncertainties of an SCWR core that includes control blades and burnable absorbers. A number of approximations were made and a number of improvement techniques have been omitted (as discussed above).

A previous SCWR lattice-level study [17], which had three fuel rings rather than two, and a central burnable absorber, reported similar sensitivities. For example, the study reports the ^{239}Pu fission sensitivity to be 0.33 at the beginning of cycle, whereas 0.31 was found in this study. These numbers are comparable and a difference is expected considering that the concentrations of plutonium in the two fuel lattice models differ. Many of the other nuclide/reactions have comparable values as well.

A control blade inserted into the KENO model is extended to the exact depth calculated by PARCS. By contrast, in PARCS, the 2 group homogenized and condensed cross sections are interpolated between the reference case (without the blade) and the branch case (with the blade), by the amount of the insertion depth. This most likely leads to significant differences in power at the region near the bottom

of the blade when a blade is partially inserted into a node. This results in spatial self-shielding effects that are not taken into account in the PARCS model.

The burnable absorbers modelled in TRITON/NEWT had 20 individual concentric rings. This was to account the outer regions of the burnable absorbers spatially self-shielding the inner regions during depletion. However, in KENO only a single pin was modelled due to the limit of KENO's memory allocation. The result is a steady decline in ^{155}Gd and ^{157}Gd concentration over the cycle in KENO's case.

It is important to point out that discrepancies between a two-group diffusion code (without using improvements such as ADF or exact cross sections) and a 238 group Monte Carlo code, are expected. Additionally, as described above, other fuel-related approximations were used in order to build a feasible KENO model. In this study we see discrepancies up to ~20 mk between PARCS and KENO. As a comparison it has been documented that discrepancies of up to 8 mk in k_∞ exist for the SCWR fuel cell between MCNP6 and DRAGON (using the IAEA library) [13]. Therefore, it is not unexpected to see such large differences at the full-core level under such approximations.

All things considered, the results presented in this study are accurate for scoping purposes and to understand important physics phenomena occurring in the SCWR core along its cycle.

5. Conclusion

A quarter-core calculation of $k_{eff} \pm \Delta k_{eff}$ which includes control blades and burnable absorbers has been reported in this study. At 0 FPD k_{eff} = 1.0134±0.0085 and at 404 FPD k_{eff} = 1.0131 ± 0.0078. These numbers, which were calculated by KENO and TSUNAMI, are quite different (by up to ~20 mk) from the numbers obtained by the diffusion code PARCS.

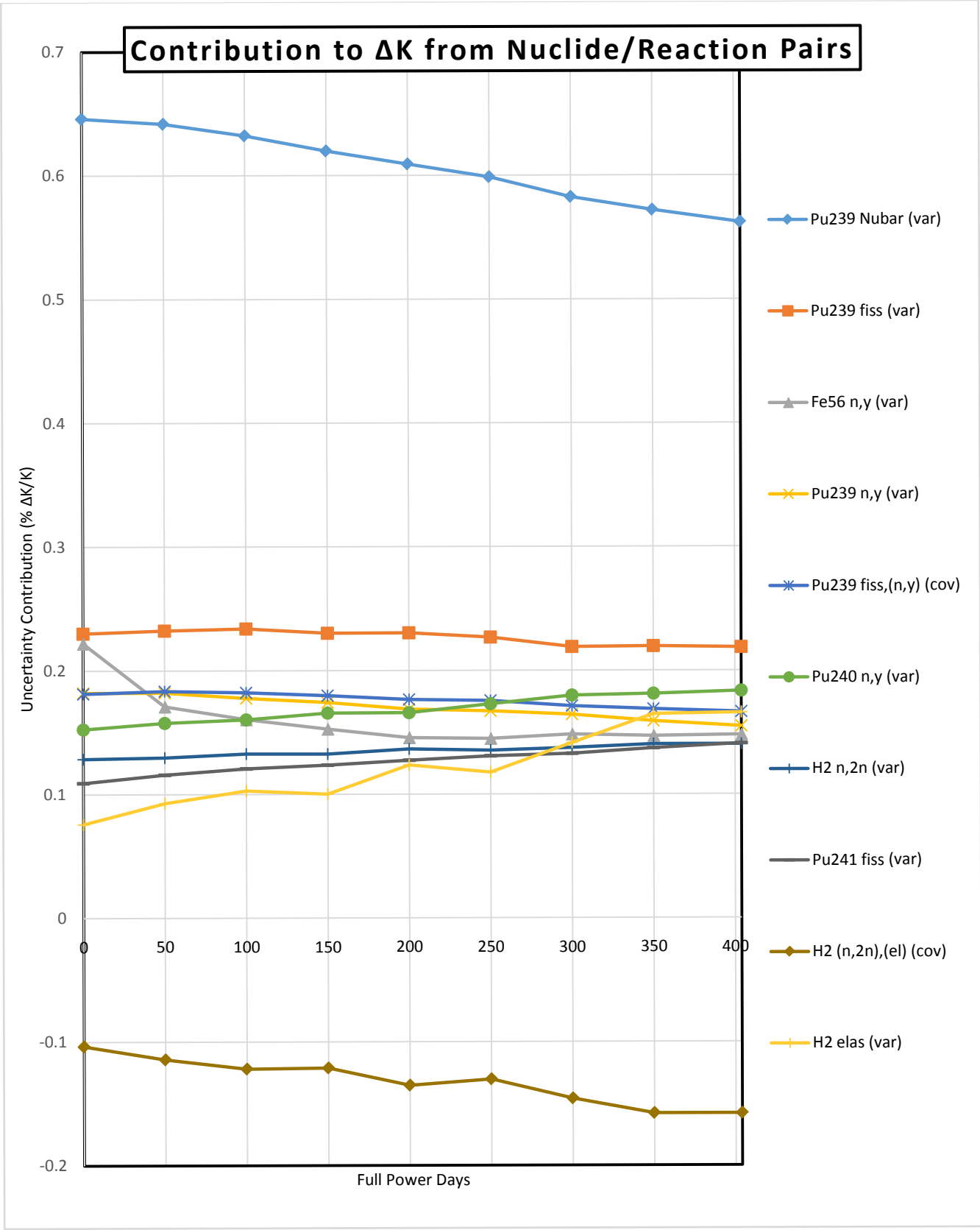
Contribution to ΔK from Nuclide/Reaction Pairs
Uncertainty Contribution (% ΔK/K)
0.7
0.6
0.5
0.4
0.3
0.2
0.1
0
-0.1
-0.2
0
50
100
150
200
250
300
350
400
Full Power Days
Pu239 Nubar (var)
Pu239 fiss (var)
Fe56 n,y (var)
Pu239 n,y (var)
Pu239 fiss,(n,y) (cov)
Pu240 n,y (var)
H2 n,2n (var)
Pu241 fiss (var)
H2 (n,2n),(el) (cov)
H2 elas (var)

Figure 7: Uncertainty contributions to k_{eff} from nuclide/reaction pairs.

Nuclides/reactions to which k_{eff} has the largest sensitivity have been reported. ^{239}Pu $\bar{\nu}$, ^{239}Pu fission, ^{241}Pu $\bar{\nu}$, and ^{241}Pu fission had the largest sensitivities. Due to the large sensitivities and significant variances, of the aforementioned plutonium nuclides/reactions, they were identified as being among the largest uncertainty contributors.

A number of physics phenomena were exposed by investigating nuclides and reactions with large changes in sensitivity over the cycle. Such as the compliment of absorption in the control blades by moderation by heavy water upon their removal which provide the control blades' reactivity worth.

Future studies will include improvements such as assembly discontinuity factors and possibly multi-cell exact cross sections. In addition, potentially more burnup compositions can be included in the fuel in the TSUNAMI model. The improved study will then be used in a cross-section adjustment and bias calculation, along the cycle, for the SCWR reactor – this will include the generation of ZED-2 experiments that can be performed to reduce the bias between SCWR simulations and experiments.

6. References

[1] B. T. Rearden and M. A. Jessee, "TSUNAMI Utility Modules," Tech. Rep. ORNL/TM-2005/39 Version 6.1 Sect. M18, Oak Ridge National Laboratory, June 2011.

[2] L. M. Petrie *et al*, "KENO V.a: An Improved Monte Carlo Criticality Program," Tech. Rep. ORNL/TM-2005/39 Version 6.1 Sect. F11, Oak Ridge National Laboratory, June 2011.

[3] Scale: A Comprehensive Modeling and Simulation Suite for Nuclear Safety Analysis and Design, ORNL/TM-2005/39, Version 6.1, June 2011. Available from Radiation Safety Information Computational Center at Oak Ridge National Laboratory as CCC-785.

[4] B. T. Rearden et al., "SAMS: Sensitivity Analysis Module for SCALE," Tech. Rep. ORNL/TM-2005/39 Version 6.1 Sect. F22, Oak Ridge National Laboratory, June 2011.

[5] M. McDonald, A. Colton and J. Pencer, "Power Flattening and Reactivity Suppression Strategies for the Canadian Supercritical Water Reactor Concept," in the 35th Annual Conference of the Canadian Nuclear Society, Saint John, NB, 2015. Paper 40

[6] F. Salaun, J. R. Sharpe, D. W. Hummel, A. Buijs and D. R. Novog, "Optimization of the PT-SCWR Control Blade Sequence using PARCS and DAKOTA," in the 7th International Symposium on Supercritical Water-Cooled Reactors, Helsinki, Finland, 2015. Paper 2073.

[7] F. Salaun, D. W. Hummel and D.R. Novog, "Preliminary Study on the Use of Burnable Neutron Absorbers in the Pressure Tube Type Super Critical Water-cooled Reactor," in the 19th Annual Pacific Basin Nuclear Conference, Vancouver, BC, 2014. Poster Submission.

[8] M. A. Jessee and M. D. DeHart, "NEWT: A New Transport Algorithm for Two-Dimensional Discrete-Ordinates Analysis in Non-Orthogonal Geometries," Tech. Rep. ORNL/TM-2005/39 Version 6.1 Sect. F21, Oak Ridge National Laboratory, June 2011.

[9] M. A. Jessee and M. D. DeHart, "TRITON: A Multipurpose Transport, Depletion, and Sensitivity and Uncertainty Analysis Module," Tech. Rep. ORNL/TM- 2005/39 Version 6.1 Sect. T1, Oak Ridge National Laboratory, June 2011.

[10] T. Downar, Y. Xu and V. Seker, "Theory Manual for the PARCS Kinetics Core Simulator Module," Version 3.0, 2012.

[11] J. Pencer, D. Watts, A. Colton, X. Wang, L. Blomeley, V. Anghel and S. Yue, "Core Neutroncs for the Canadian SCWR Conceptual Design," in the 6th International Symposium on Supercritical Water-cooled Reactors, Shenzhen, Guangdong, China (2013).

[12] W. Shen, "Assessment of the Traditional Neutron-diffusion Core-analysis Method for the Analysis of the Super Critical Water Reactor," *Ann; Nucl. Energy*, **45**, 1-7 (2012).

[13] J. R. Sharpe, F. Salaun, D. Hummel, A. Moghrabi, M. Nowak, J. Pencer, D. Novog and A. Buijs, "A Benchmark Comparison of the Canadian Supercritical Water-cooled Reactor (SCWR) 64-element Fuel Lattice Cell Parameters using Various Computer Codes," in the 35th Annual Conference of the Canadian Nuclear Society, Saint John, NB (2015).

[14] J. R. Sharpe, A.Buijs and J. Pencer, "Methodology to Design Simulated Irradiated Fuel by Maximizing Integral Indices (c_k, E, G)," *ASME J. Nuclear. Rad. Sci.*, **2**, 021017-1 (2016).

[15] B. T. Rearden, "TSUNAMI-3D: Control Module for Three-dimensional Cross-section Sensitivity and Uncertainty Analysis for Criticality," Tech. Rep. ORNL/TM- 2005/39 Version 6.1 Sect. C9, Oak Ridge National Laboratory, June 2011.

[16] Data produced using the Online Service retrieval code package written by C. L. Dunford, National Nuclear Data Center, Brookhaven National Laboratory.

[17] L. Blomeley, J. Pencer, B. Hyland and F. P. Adams, "Nuclear Data Sensitivity and Uncertainty for the Canadian Supercritical Water-cooled Reactor," *Ann. Nucl. Energy*, **63**, 587-593 (2014).